Noel, J. P., Renson, L., Kerschen, G., Peeters, B., Manzato, S., & Debille, J. (2014). Nonlinear Dynamic Analysis of an F-16 Aircraft Using GVT Data. In *International Forum on Aeroelasticity and Structural Dynamics (IFASD 2013): Proceedings of a meeting held 24-26 June 2013, Bristol, United Kingdom* (Vol. 1, pp. 990-1002). Royal Aeronautical Society.

Peer reviewed version

NONLINEAR DYNAMIC ANALYSIS OF AN F-16 AIRCRAFT USING GVT DATA

J.P. Noël[1], L. Renson[1], G. Kerschen[1], B. Peeters[2], S. Manzato[2], J. Debille[2]

[1] Space Structures and Systems Laboratory
Aerospace and Mechanical Engineering Department
University of Liège
Chemin des chevreuils 1, B-4000, Liège, Belgium
jp.noel, l.renson, g.kerschen@ulg.ac.be

[2] LMS International
Interleuvenlaan 68, B-3001, Leuven, Belgium
bart.peeters, simone.manzato, jan.debille@lmsintl.com

Keywords: Characterisation of structural nonlinearities; F-16 aircraft; GVT data.

Abstract: This paper aims at investigating the nonlinear dynamics of an F-16 aircraft, based upon sine-sweep data collected during a ground vibration test campaign. Various analysis techniques, including the mere visual inspection of the time series, the wavelet transform and the restoring force surface method, are utilised and reveal that the F-16 wing-to-payload mounting interfaces exhibit both softening and hardening nonlinearities.

1 INTRODUCTION

Aircraft structures are known to be prone to nonlinear phenomena, especially today as they become lighter and hence more flexible. A specific challenge encountered with fighter aircraft, besides aeroelastic nonlinearity [1], is the modelling of the wing-to-payload mounting interfaces. Indeed, for large amplitudes of vibration, they may trigger complex nonlinear mechanisms such as friction or gaps. This usually translates into a decrease of certain resonance frequencies for increasing force levels that cannot be observed for linear structures [2]. In this context, the present work intends to investigate the nonlinear dynamics of an F-16 aircraft, based upon experimental data collected during a ground vibration test (GVT) campaign.

The objective of this paper is specifically to exploit high-level sine-sweep data and demonstrate that they can provide useful insight towards accurately modelling nonlinear behaviour. Various analysis techniques, including the mere visual inspection of the time series, the wavelet transform and the restoring force surface method, will be utilised to bring different perspectives to the F-16 dynamics, which will be shown to exhibit both softening and hardening nonlinearities.

2 F-16 INSTRUMENTATION AND FREQUENCY RESPONSE FUNCTION-BASED ANALYSIS

Experimental data addressed in this study were recorded on a full-scale F-16 aircraft (Figure 1 (a)) on the occasion of the LMS Ground Vibration Testing Master Class [3] held in September 2012 at the Saffraanberg military basis in Belgium. During the test campaign, the aircraft was equipped with two dummy payloads mounted at wing tips (Figure 1 (b)) and one dummy store connected through a pylon to the left wing (Figure 1 (c)). The structure was suspended in free-free conditions using bungee chords and air suspension systems, and two shakers were attached underneath the two wings so that both wing bending and torsion modes could be excited (Figure 1 (d)). The aircraft was extensively instrumented by means of 45 uniaxial and 40 triaxial accelerometers, thus yielding 165 measured degrees of freedom. In particular, triaxial sensors were positioned on both sides of the wing-to-payload and wing-to-store connections, as these latter are known to be potential sources of nonlinearity (Figure 1 (e)). The connections between the wings and the flaps and between the vertical tail and the rudder were similarly instrumented, even if the control surfaces were held fixed throughout the tests.

Figure 2 charts the stabilisation diagram calculated by the PolyMAX method [4] using random data measured at low level, *i.e.* considering a root-mean-squared (RMS) force amplitude of 8 N. This diagram leads to the identification of 3 rigid-body modes located below 4 Hz and 5 flexible modes, whose estimated frequencies and damping ratios are listed in Table 1. The first rigid-body mode, which involves a roll movement of the structure, together with the deformed shapes of the flexible modes are depicted in Figures 3 (a – f), respectively. A frequency response function (FRF) measured on the right wing leading edge is also plotted in Figure 2 and shows very good agreement with the columns of stabilised poles.

Besides providing the basis for most frequency-domain modal parameter estimation techniques, such as the PolyMAX method, FRFs can also be exploited for detecting nonlinearity. Indeed, if the system under test is linear, they are required to be independent of the force amplitude spectrum. The comparison of FRFs for different input levels is therefore a reliable indicator of the presence of nonlinear behaviour in specific frequency bands [5]. This comparison, often referred to as the homogeneity test, is arguably one of the most popular detection tools [6], by virtue of the fact that almost all the commercial spectrum analysers allow the straightforward display of FRF plots. This analysis is herein achieved in Figures 4 (a – b) for FRFs measured on the right wing leading edge and the aircraft nose, respectively, and for input levels of 8, 32 and 54 N RMS. In the two graphs, the rigid-body modes show no dependence upon the input level, whereas all the flexible modes are found to be affected by substantial softening distortions, which are the clear evidence of the activation of nonlinearity.

However, although it proves convenient for nonlinearity detection, the homogeneity test does convey no information about the nature of the nonlinearity sources, other than the global softening or hardening behaviour of the resonance peaks. One notes that the odd or even nature of the nonlinearities can also be revealed as described in [7], but the procedure requires advanced random excitation signals, which are generally not available during a typical GVT campaign. In this context, the use of sine-sweep data is a relevant alternative that is investigated in the next section.

(a) Overall view of the F-16.

(b) Dummy payload mounted at the right wing tip.

(c) Dummy store connected to the left wing.

(d) Shaker attached underneath the left wing.

(e) Potential nonlinear connection instrumented on both sides.

Figure 1: Full-scale F-16 aircraft tested during the LMS GVT Master Class.

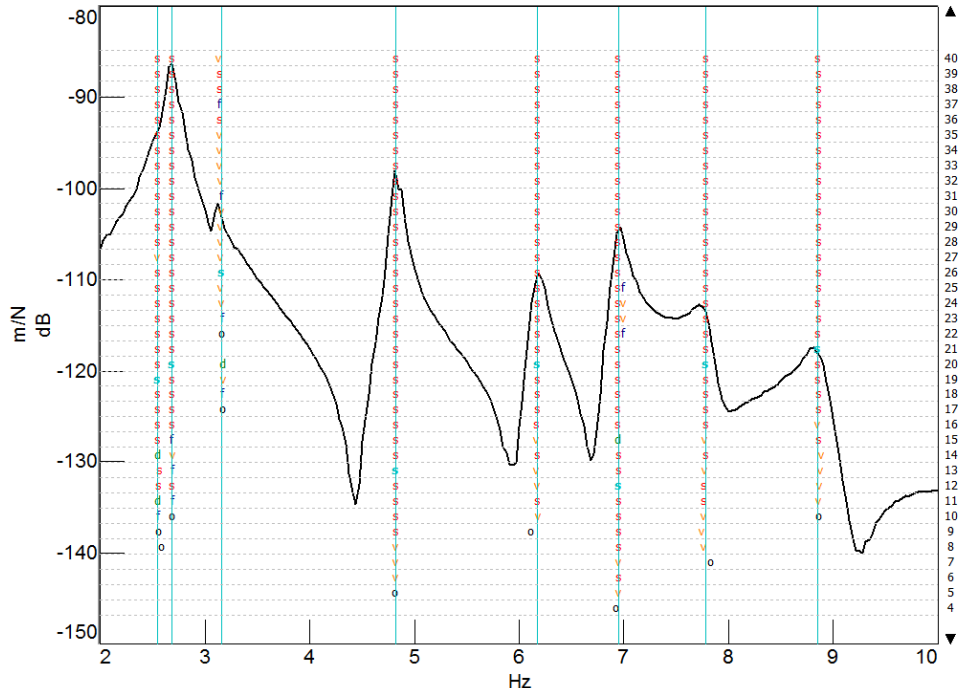

Figure 2: Stabilisation diagram computed using the PolyMAX method for model orders up to 40, and FRF measured on the right wing leading edge.

Mode	Frequency (Hz)	Damping ratio (%)
1	4.82	0.74
2	6.18	0.98
3	6.95	0.72
4	7.78	1.25
5	8.85	1.37

Table 1: Frequencies and damping ratios of the flexible modes up to 10 Hz estimated using the PolyMAX method.

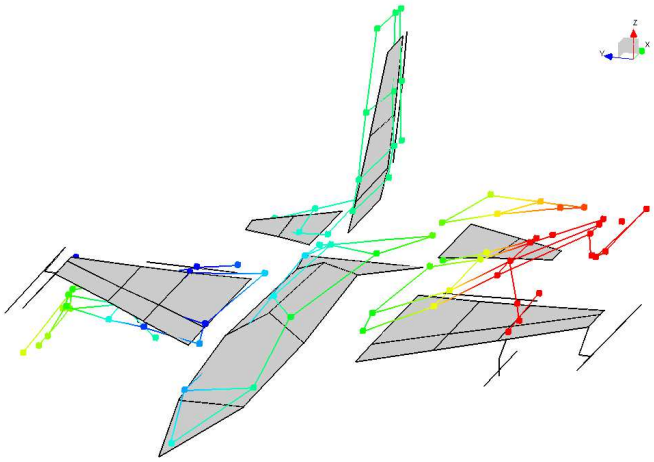

(a) First rigid-body mode at 2.50 Hz: roll movement.

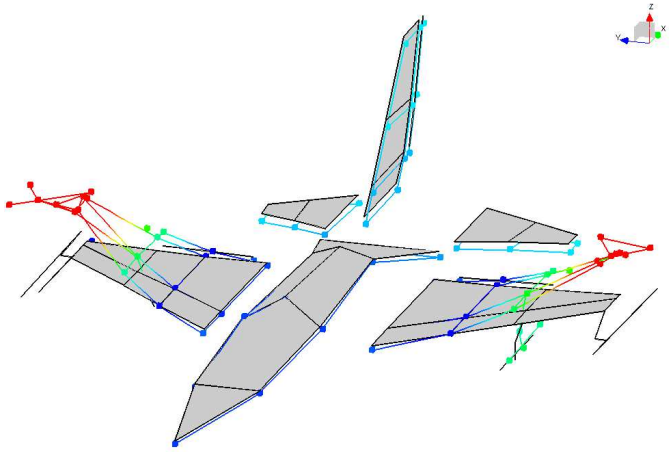

(b) First mode at 4.82 Hz: wing bending.

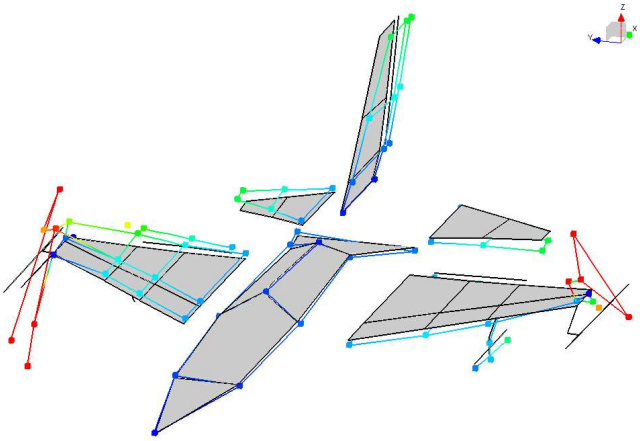

(c) Second mode at 6.18 Hz: antisymmetric payload rotation.

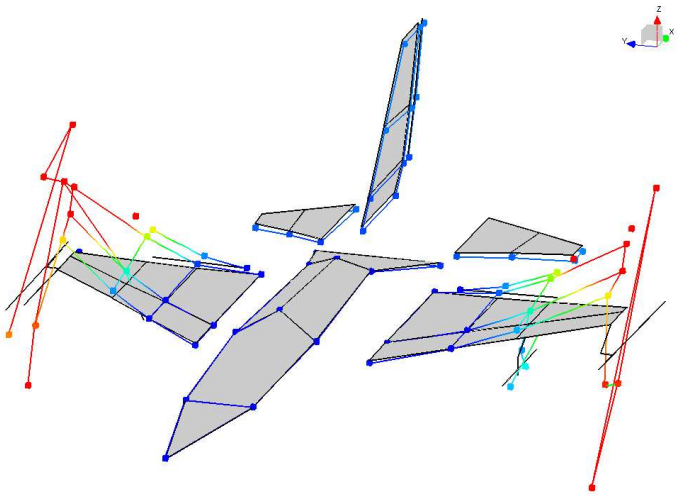

(d) Third mode at 6.95 Hz: symmetric wing torsion.

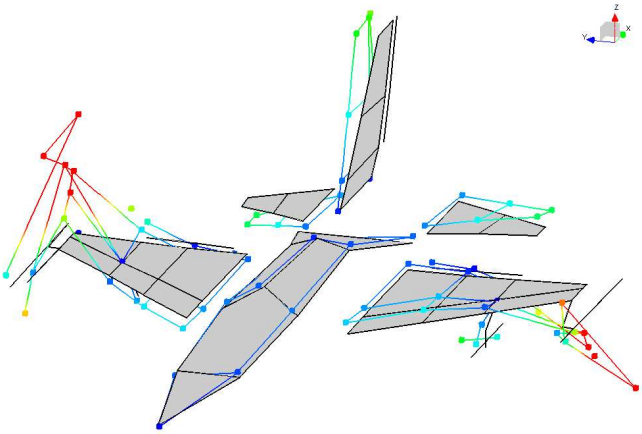

(e) Fourth mode at 7.78 Hz: antisymmetric wing torsion.

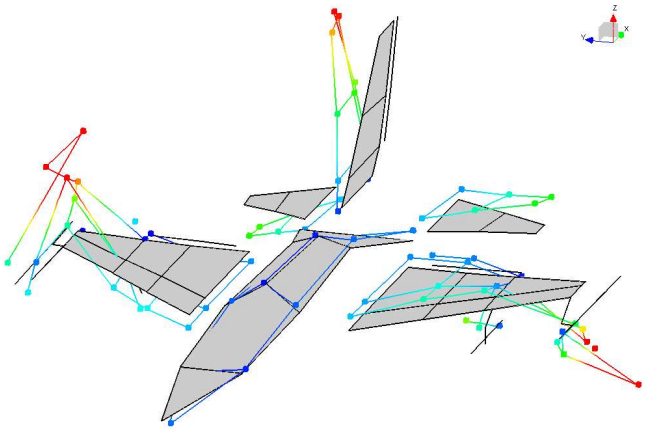

(f) Fifth mode at 8.85 Hz: antisymmetric wing torsion and vertical tail bending.

Figure 3: First rigid-body mode and deformed shapes of the flexible modes up to 10 Hz estimated using the PolyMAX method.

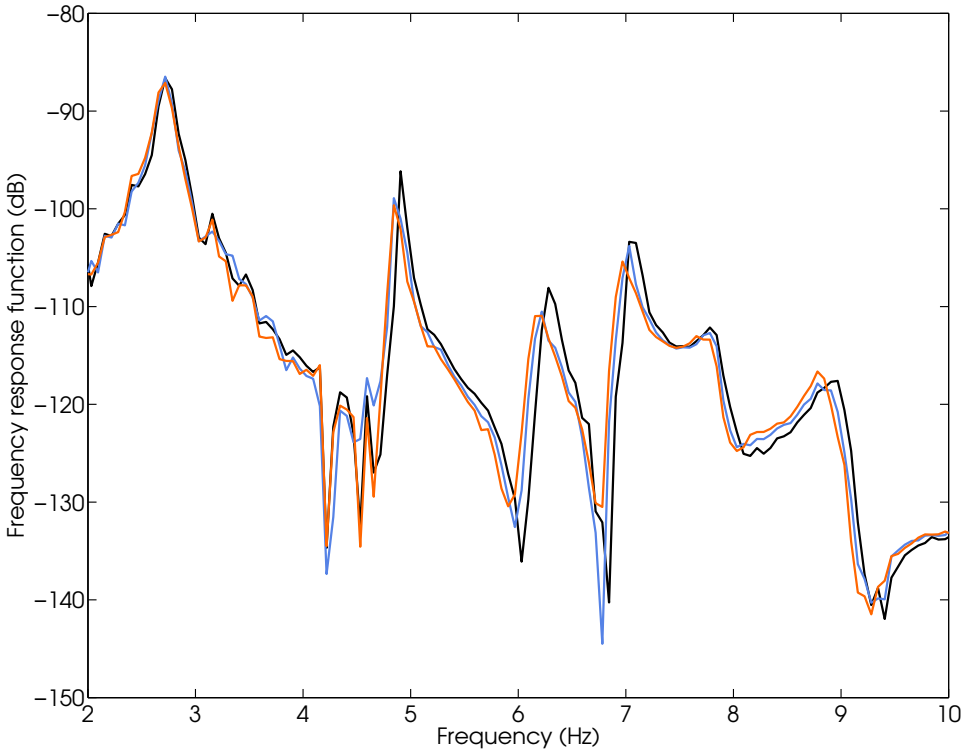

(a)

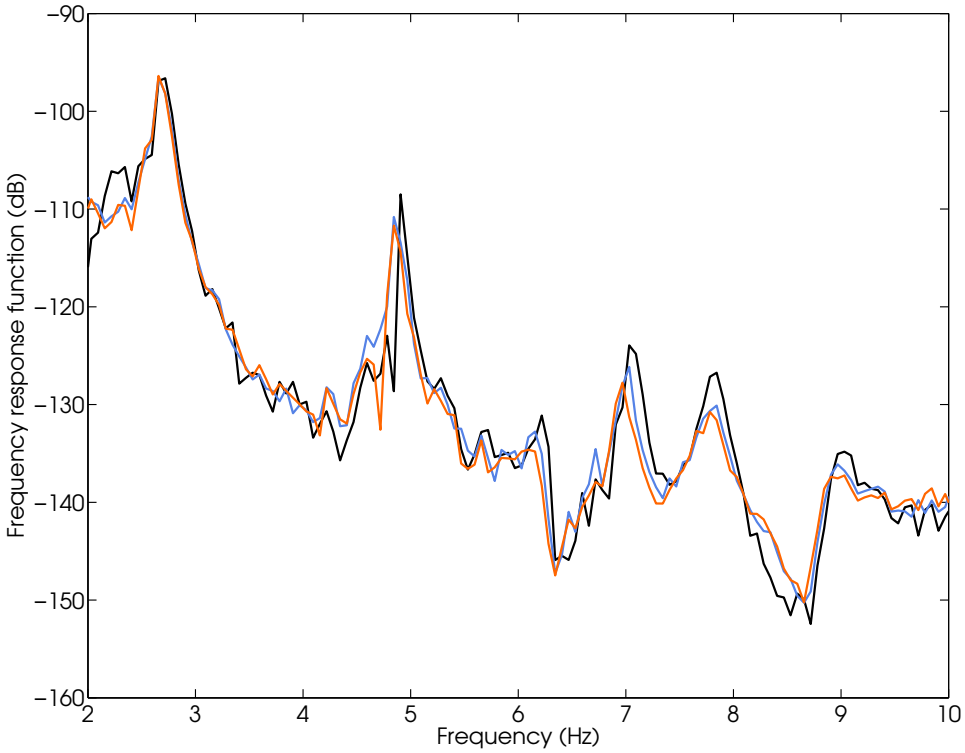

(b)

Figure 4: FRFs measured on (a) the right wing leading edge and on (b) the aircraft nose for 3 excitation levels. Black: 8 N RMS; blue: 32 N RMS; orange: 54 N RMS.

3 EXPLOITATION OF SINE-SWEEP DATA FOR NONLINEARITY CHARACTERISATION

The objective of this section is demonstrate that high-level sine-sweep data can provide useful insight towards accurately modelling the nonlinearities detected using the homogeneity test. To this end, measurements collected during an increasing and linear 54-N-sweep of the interval from 2.1 to 15.1 Hz are considered. For the sake of conciseness, we will restrict our scope to the analysis of the first wing bending mode of the structure located around 4.8 Hz, as it was found to involve significant nonlinear effects in Figures 4 (a – b), but also large displacements at the payload mounts and hence good signal-to-noise ratios.

3.1 Visual inspection of the raw time series

A distinct property of nonlinear systems is their ability to generate harmonic components, which can be exploited to gain knowledge into the nonlinear mechanisms involved. In this regard, sine-sweep excitations are particularly convenient because, if linear, the structure is known to generate a pure sine wave in output. Harmonic distortions can sometimes be such that a mere visual inspection of the raw time series is sufficient to reveal nonlinear behaviour. For that purpose, the accelerations measured on the dummy payload mounted to the right wing and on the dummy store are plotted versus sweep frequency in Figures 5 (a – b), respectively. The connections between the left wing and the payload, the wings and the flaps, and the vertical tail and the rudder are not studied herein because they exhibit much less marked nonlinear behaviours.

The two resonance envelopes corresponding to the first wing bending mode at 4.8 Hz in Figures 5 (a – b) show no clear evidence of nonlinearity. However, a close-up analysis in 4.6 – 5.4 Hz, as achieved in Figures 5 (c – d), reveals the presence of harmonics in the vicinity of resonance. These harmonics are better highlighted in Figures 5 (e – f), where a few cycles only are studied. Sudden dips can be observed in the oscillations in Figure 5 (e) for large accelerations, which are the symptom of a non-smooth decrease of stiffness in the system. By contrast, the presence of shocks in Figure 5 (f) is an indication of a non-smooth but hardening nonlinearity.

3.2 Time-frequency analysis using the wavelet transform

The Fourier transform (FT), which maps the time-domain signal $x(t)$ onto its frequency-domain representation $X(\omega)$ as

$$X(\omega) = \int_{-\infty}^{\infty} x(t)\, e^{-j\omega t}\, dt\,, \tag{1}$$

is widely used in structural dynamics for various purposes. One of its main limitations is that it is not suitable for the analysis of nonstationary signals. These signals see their frequency content evolving with time and are characteristics of nonlinear systems.

An improvement of the classical FT is the short-time Fourier transform (STFT). The signal to be analysed is multiplied by a window function $w(t)$ which is nonzero for only a

short period of time. The FT of the resulting signal is taken as the window is slid along the time axis, resulting in a two-dimensional representation $X(\omega, \tau)$ of the signal

$$X(\omega, \tau) = \int_{-\infty}^{\infty} x(t)\, w(t-\tau)\, e^{-j\omega t}\, dt\,. \tag{2}$$

The inherent problem of the STFT is that the window is not adjustable, and a wide (narrow) window thus gives good (poor) frequency resolution but poor (good) time resolution.

The fixed resolution of the STFT motivated the development of advanced time-frequency analysis methodologies such as the wavelet transform (WT). Unlike the STFT, the WT involves a windowing technique with variable-sized regions:

$$X_\psi(a, b) = \frac{1}{\sqrt{a}} \int_{-\infty}^{\infty} x(t)\, \psi\left(\frac{t-b}{a}\right)\, dt \tag{3}$$

where variable b locates the observation window in the time domain, and variable a contracts or expands the window. It has the advantage that small time intervals are considered for high-frequency components, whereas the size of the interval is increased for lower-frequency components, thereby yielding better time and frequency resolutions than the STFT. This makes the WT one of the more versatile tools for interpreting harmonic components generated by nonlinear systems [8]. The Morlet mother wavelet, which is a Gaussian-windowed complex sinusoid $\psi(t) = e^{-t^2/2}\, e^{-j\omega t}$, is considered herein.

The wavelet amplitudes of the accelerations of Figures 5 (a – b) are displayed in logarithmic scaling in Figures 6 (a – b), respectively. The presence of multiple odd and even harmonics around 5 Hz in Figure 6 (a) is a confirmation of the non-smooth nature of the wing-to-payload nonlinearity. One also remarks the particularly significant amplitudes of the seventh and eighth harmonics, which are likely to underlie interactions between nonlinear modes of vibration [9]. Figure 6 (b) indicates that the nonlinearity in the wing-to-store pylon is also non-smooth. The wavelet amplitude additionally reveals that this latter greatly impacts the symmetric wing torsion mode around 7 Hz. One finally notes that the higher acceleration levels reached in Figure 5 (a) result in a better signal-to-noise ratio in Figure 6 (a).

3.3 Restoring force surface method

The restoring force surface (RFS) method [10] relies on Newton's second law of motion, written for a single-degree-of-freedom system as

$$m\,\ddot{x} + f(x, \dot{x}) = p \tag{4}$$

where m is the mass, $\ddot{x}$ the acceleration and p the external force and where f encompasses all the restoring forces in the system, being of elastic or dissipative nature. This equation recast into

$$f(x, \dot{x}) = p - m\,\ddot{x} \tag{5}$$

gives a direct access to the restoring force surface defined by the triplets (x_i, $\dot{x}_i$, f_i), where i refers to the i-th sampled instant. Moreover, cross sections of this restoring force surface along the axes where either the velocity or the displacement is equal to zero yield stiffness

and damping curves and allow the characterisation of the elastic and dissipative forces, respectively. Applied to more complex systems, as in the case of the F-16, the RFS method only provides qualitative information, but can still be exploited for visualising nonlinear effects by representing the inertia force of one nonlinear component versus the relative displacement or velocity across this component.

The force-displacement curve of the right-wing-to-payload connection is drawn in Figure 7 (a) for sweep frequencies between 4.6 and 5.4 Hz. A sudden loss of stiffness is observed beyond a relative displacement of about 2.7 mm, which can be confidently attributed to the opening of the connection for sufficiently high forcing amplitudes. This also explains the softening behaviour of the resonance peaks observed in Figures 4 (a – b) and the acceleration dips visible in Figure 5 (a). The force-displacement curve computed across the left-wing-to-store connection is depicted in Figure 7 (b) and shows a completely different behaviour. Indeed, a severe increase of stiffness is observed which corresponds to impacts onto a displacement-limiting component in the mounting interface, and is in line with the observations made based upon Figures 5 (f) and 6 (b). The associated clearances are found to be symmetric and can be estimated at 0.065 mm. This hardening behaviour is however not visible in the FRFs plotted in Figures 4 (a – b), as it is dominated by the softening effect evidenced in Figure 7 (a) which involves larger restoring force values.

4 CONCLUSION

The objective of this paper was to address the characterisation of the structural nonlinearities of a full-scale F-16 aircraft equipped with two dummy payloads and one dummy store. For that purpose, robust methods, namely the mere visual inspection of the time series, the wavelet transform and the restoring force surface method, were applied to experimental data recorded during a typical GVT campaign. Specifically, high-level sine-sweep data were proved to be particularly well suited to acquire a precise understanding of the nonlinear mechanisms involved. The mounting interface between the right wing tip and a dummy payload was thus found to loosen at high excitation amplitude and to trigger the decrease of the resonance frequencies of the structure. Moreover, the existence of a clearance within the pylon between the dummy store and the left wing was also evidenced, and was shown to translate into impacts in the aircraft response.

ACKNOWLEDGEMENTS

The authors J.P. Noël and L. Renson are Research Fellows (FRIA fellowship) of the *Fonds de la Recherche Scientifique – FNRS* which is gratefully acknowledged.

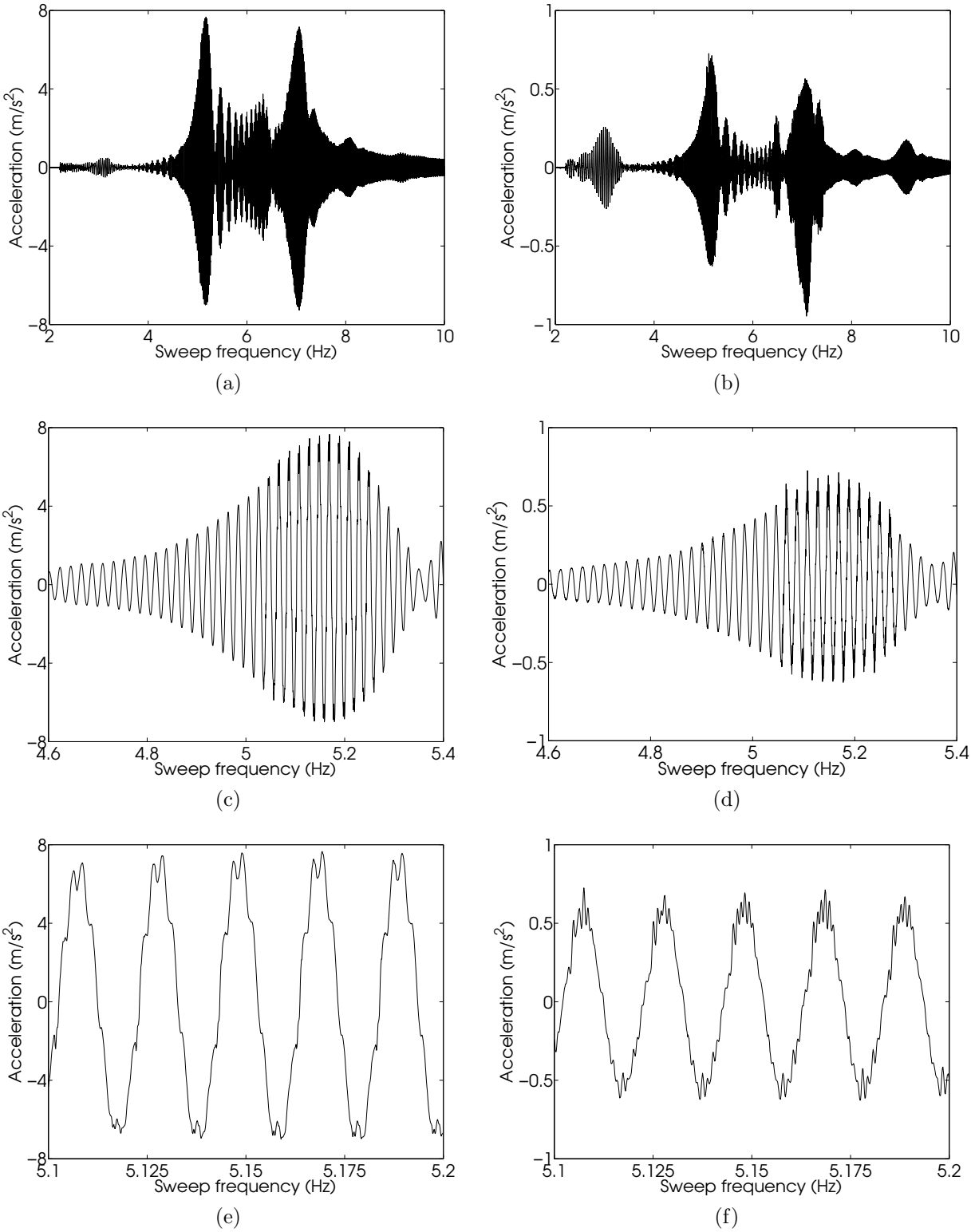

Figure 5: Accelerations measured on the dummy payload mounted to the right wing (left column) and on the dummy store (right column) for 3 sweep frequency intervals. (a – b) 2 – 10 Hz; (c – d) 4.6 – 5.4 Hz; (e – f) 5.1 – 5.2 Hz.

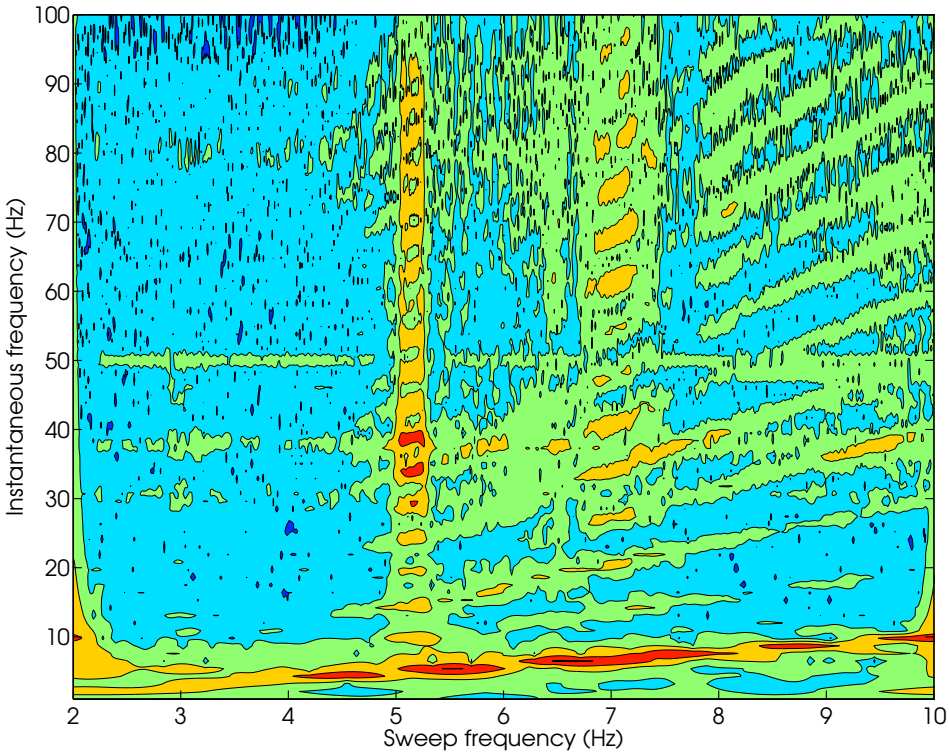

(a)

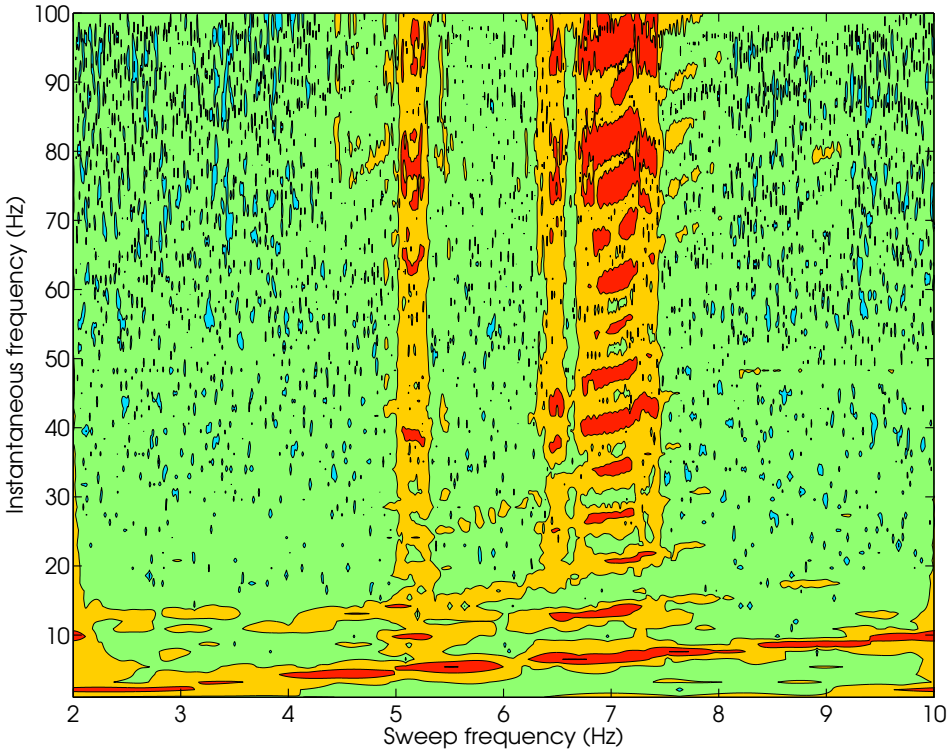

(b)

Figure 6: Wavelet transform amplitudes (in logarithmic scaling) of the accelerations measured on (a) the dummy payload mounted to the right wing and on (b) the dummy store. Colour map goes from blue to red, which correspond to low (-300 dB) amplitude and high (0 dB) amplitude regions, respectively.

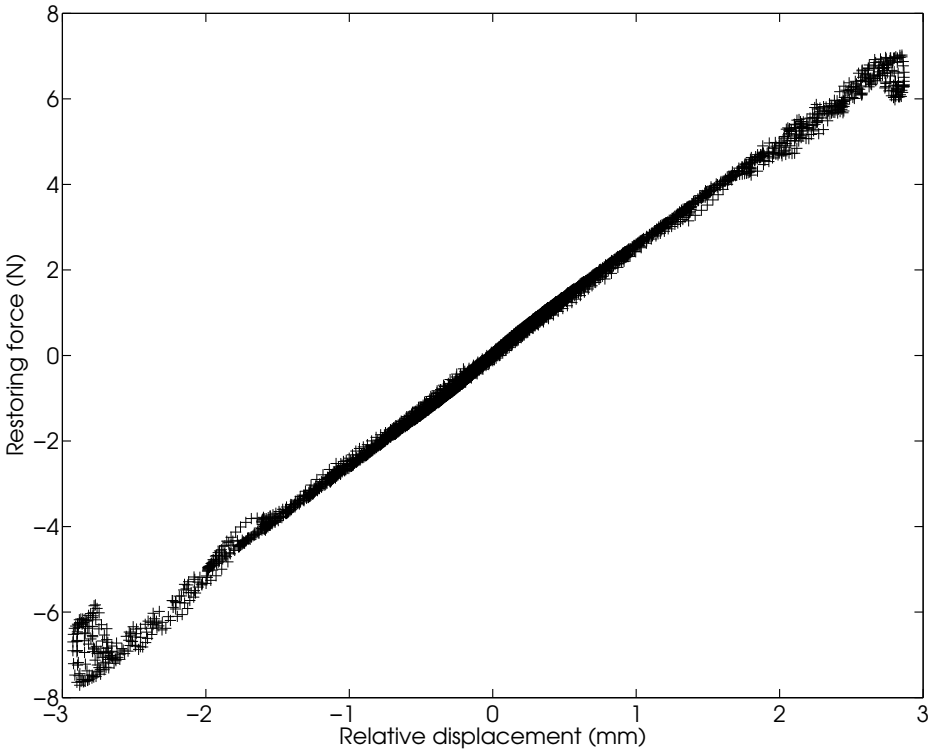

(a)

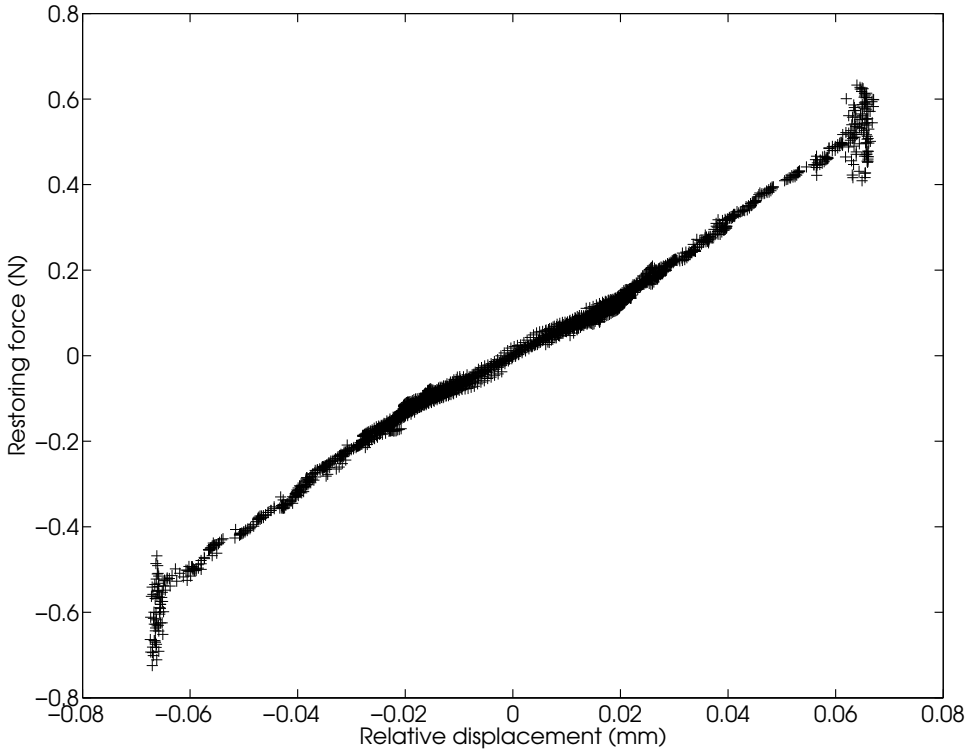

(b)

Figure 7: Force-displacement curves across (a) the right-wing-to-payload connection and (b) left-wing-to-store connection computed using the RFS method.

5 REFERENCES

[1] Denegri Jr., C. M. (2000), Limit cycle oscillation flight test results of a fighter with external stores, Journal of Aircraft, 37(5), 761-769.

[2] Ahlquist, J. R., Carreo, J. M., Climent, H., de Diego, R., and de Alba, J. (2010), Assessment of nonlinear structural response in A400M GVT, In the Proceedings of the International Modal Analysis Conference, Jacksonville, FL.

[3] Lau, J., Peeters, B., Debille, J., Guzek, Q., Flynn, W., Lange, D. S., and Kahlmann, T. (2011), Ground Vibration Testing Master Class: modern testing and analysis concepts applied to an F-16 aircraft, In the Proceedings of the International Modal Analysis Conference, Jacksonville, FL.

[4] Peeters, B., Van der Auweraer, H., Guillaume, P., and Leuridan, J. (2004), The PolyMAX frequency-domain method: a new standard for modal parameter estimation ?, Shock and Vibration, 11, 395-409.

[5] Kerschen, G., Worden, K., Vakakis, A. F., and Golinval, J.C. (2006), Past, present and future of nonlinear system identification in structural dynamics, Mechanical Systems and Signal Processing, 20, 505-592.

[6] Peeters, B., Carrella, A., Lau, J., Gatto, M., and Coppotelli, G. (2011), Advanced shaker excitation signals for aerospace testing, In the Proceedings of the International Modal Analysis Conference, Jacksonville, FL.

[7] Pintelon, R., and Schoukens, J. (2001), System identification: a frequency domain approach, Wiley-IEEE Press, New Jersey.

[8] Staszewski, W. J. (2000), Analysis of non-linear systems using wavelets, Proceedings of the Institution of Mechanical Engineers Part C – Journal of Mechanical Engineering Science, 241(11), 1339-1353.

[9] Noël, J.P., Renson, L., and Kerschen, G. (2013), Experimental identification of the complex dynamics of a strongly nonlinear spacecraft structure, In the Proceedings of the ASME International Design Engineering Technical Conference, Portland, OR.

[10] Masri, S. F., and Caughey, T. K. (1979), A nonparametric identification technique for nonlinear dynamic problems, Journal of Applied Mechanics, 46, 433-447.